CONF-8810321--1

Received by OSTI
FEB 24 1989

ORDER IN COLD IONIC SYSTEMS: DYNAMIC EFFECTS*

CONF-8810321--1

DE89 007377

John P. Schiffer

Argonne National Laboratory, Argonne, IL 60439-4843

The present state and recent developments in Molecular Dynamics calculations modeling cooled heavy-ion beams are summarized. First, a frame of reference is established, summarizing what has happened in the past; then the properties of model systems of cold ions studied in Molecular Dynamics calculations are reviewed, with static boundary conditions with which an ordered state is revealed; finally, more recent results on such modelling, adding the complications in the (time-dependent) boundary conditions that begin to approach real storage rings (ion traps) are reported.

*This research was supported by the U. S. Department of Energy, Nuclear Physics Division, under Contract W-31-109-Eng-38.

INTRODUCTION

Table I shows a summary of the history of the subject. Early pioneering work at the beginning of this century focused on understanding crystal lattices in general, the mathematical properties associated with crystal lattices, and of electrolytes [1]. Wigner's contribution to the quantum-mechanical understanding of electrons in alkali metals [2] showed the first indication of favoring bcc symmetry, in a Coulomb crystal, and such systems are often referred to as "Wigner crystals" in the literature. Detailed studies of classical Coulomb gases (One Component Plasmas or OCPs) became possible with the advent of computers -- the properties of infinite Coulomb gases were explored theoretically in the 1960-s and '70-s [3,4]. It was found that an infinite OCP undergoes a phase transition to a body-centered cubic solid at $\Gamma \simeq 170$,

$$\Gamma = (q^2/a) \ / \ (kT),$$

where $a \equiv (4/3\ \rho)^{-1/3}$ and ρ is the particle density.

The possibility of achieving cold ionic systems in trapped charged particles has been the subject of speculations. Three years ago, Paul Kienle and I became interested in the possibility of reaching this state in storage rings for heavy ions [5]. The principal point was that the coupling parameter Γ, will have particularly large values for highly charged beams, confined in the focusing field of a storage ring and cooled to a low temperature in the moving frame.

The investigation of the properties of such externally confined cold OCP systems [6] was started in collaboration with a long term colleague and friend, the late Aneesur Rahman. Rahman was one of the pioneers of the calculational technique called Molecular Dynamics, which seems ideally suited to such a problem. In this method, the Hamiltonian for the interaction between particles and the external boundary conditions is solved explicitly; it makes excellent use of the computational power of modern supercomputers.

The focusing and space-charge forces on a particle beam, regarded as a uniformly charged tube of particles, are shown in Figure 1. The focusing force is represented by a constant (harmonic) force (representing a first idealization to the real focusing lattice of a storage ring in the co-moving frame), that is proportional to the displacement of a particle from an axis. If the particles have small thermal energies then this focusing force will be balanced by the repulsive space-charge forces, and there is no net macroscopic force on the particles inside the tube -- only residual two-particle interactions will play a significant role.

STATIC SYSTEMS

The results of some of the first MD calculations [6] of such a confined system showed a surprising difference from an infinite OCP: not only were the particles arranged in the form of a tube, but they formed well-defined layers: concentric shells, with the particles within each shell arranged in a hexagonal lattice that is characteristic of two-dimensional Coulomb systems. These patterns are shown in Figures 2 and 3.

Two-dimensional Confinement

The radial size of these cold systems grows gradually with particle number. We may define λ as the number of particles per unit length ("a" defined above). At low λ the particles do not repel each other sufficiently and sit on the axis. Above λ of ~0.7 they push each other away from the axis to a finite radius, forming a series of different patterns. Some of the patterns that show up in the MD calculations are shown in Figure 4, plotted as if on the mantle of a cylinder with appropriately increasing radius. The approximate hexagonal arrangement shows up rather quickly, and various helical patterns appear as the number of hexagons per turn increases. These helical patterns have been studied further analytically [7]. At $\lambda \simeq 3.1$, the radius of the cylinder has reached a value sufficiently large that some particles start appearing on the axis; as λ increases yet further these start forming a second inner cylindrical layer. The number of cylindrical shells has been found empirically to be $N_s \simeq 0.8\ \lambda^{1/2}$. These systems will be discussed in more detail in the following talks. The shell structure does not appear at a well defined temperature, but emerges gradually, as may be seen from the beam profiles at different temperatures in Figure 5. Previous discussion of such a cold beam gave no indication of layered structures (e.g. Fig. 4.11 of Ref. 8).

Three-dimensional Confinement

The property of confined ionic systems to form an outer layer parallel to an equipotential surface, with parallel layers on the inside, seems to be quite general [9]. For a three-dimensionally isotropic confining force, one gets spherical shells as is shown in Figure 6, again with hexagonal order in each shell. With few particles [10], isotropic confinement produces the geometrical shapes shown in Figure 7, simple patterns at a fixed distance from the origin (note that these shapes are not necessarily trivial, for instance the minimum configuration for eight particles is not a cube, as was predicted by some). A new particle first appears in the center for a system with 13 particles, a second one for 20, and these gradually grow into a new central object. The number of spherical shells is given by the empirical relationship $N_s = (N/4)^{1/3}$, where N is the total number of particles.

All these systems have in common the layered structures and the hexagonal pattern within the layers. When one tries to determine how particles in the different layers arrange themselves with respect to each other, the correlation function suggests an approximate bcc pattern. Yet the hexagonal arrangement within the shells does not map into a bcc lattice -- so the two symmetries must be approximate and these structures have mixed, approximate symmetries. Even with a one-dimensional confining field a system of plane layers is formed perpendicular to the confining force. The ratio of spacings seen with one, two and three-dimensional structures are shown in Table 2, and compared to the spacings in similar planes in bcc and fcc lattices.

If the confining forces are spatially anisotropic, similar structures are obtained, elliptically or spheroidally deformed, as is seen in Figure 8.

DYNAMIC EFFECTS

Forces Between Layers

Some tests have been run in MD models on the friction between these layers [9]; the qualitative results are summarized in Figure 9. One layer (the second from the outside) was given a velocity with respect to the others, and its subsequent motion was followed in time. The motion appears to proceed essentially unhindered if it is a rotation in a curved direction, but it encounters a combination of elastic and inelastic barriers if it is along a straight direction. The fact that the particles cannot interlock in the curved directions, while they do so along straight directions may be the qualitative reason for this. These effects are interesting, though their application to ion beams does not seem to be immediate. More likely may be application to the rotating layered spheroidal clouds seen recently in Penning traps [11].

Radial Breathing Mode in Beams

In the radial direction there are definite elastic constants, and radial oscillations can be induced [12]. Such a mode may be studied in MD models by turning off the focusing force for a short interval of time in a previously equilibrated system, and then following the subsequent behavior of the average radius; an example is shown in Figure 10. The frequency of this mode is different from the betatron oscillation (the motion of a single isolated particle in the focusing field) because the effect of space charge plays an important role. Empirically the frequency seems constant at $\sqrt{2}$ times the betatron frequency and independent of the particle density, as is shown in Figure 11. Although the dissipation of this mode has not been studied carefully, it is clearly small on the time scale of many betatron periods. For a very low density beam, where the particles approach a straight line configuration, the oscillation becomes the betatron motion, but in the excursions in the absolute value of the radius, the quantity plotted in Fig. 11, this is half the betatron period.

Radial Shape Mode in Beams

Another mode is the one induced when the focusing is turned off for a short interval in only one dimension. Since space-charge effects couple the horizontal and vertical size of the beam, this induces a shape oscillation in the beam envelope that also persists for long times with a period that is very close to the betatron period, and that is also rather independent of particle number as is seen in Figure 11. At low particle densities, where space-charge effects become small, there is no coupling between the horizontal and vertical motion and this mode disappears.

Temperature Dependence of Radial Modes

These radial modes may be relatively easy to detect with standard diagnostic tools. The dependence of these modes on temperature was investigated using the different temperature systems whose profiles were shown in Figure 5. The hottest beam with $\Gamma = 0.2$ would correspond to a value of $\Delta p/p = 5 \times 10^{-5}$ for 200 MeV/u uranium. The dependence of these frequencies on temperature is shown in Figure 12, and it is clear that these modes first appear at a temperature that is perhaps two orders of magnitude higher than where the shells first become distinct. The frequencies are stabilized as soon as the beams become space-charge limited, long before the segregation into cylindrical layers occurs.

Shear Oscillations

The fact that the particles in a beam are contained in a storage ring and have to follow a closed path, means that for a pair of particles travelling side by side at the same velocity, the outer one is at a slightly larger radius and will lag behind its inner neighbor. The motion along a closed path therefore introduces a shear in the beam and the question to be investigated is the strength of the elastic constant against such shear: whether the ordered system of particles can withstand the shear or not. A cold system was therefore prepared to equilibrium and then subjected to a short pulse of shear; subsequently the system was followed in time to determine the frequency of its shear oscillations, as shown in Figure 13. Since the period of the driving force for shear in a real system is fixed by the cyclotron frequency, and the parameter scaling the calculated system is the focusing field that is represented by the betatron frequency, the question becomes whether the elastic constant for such shear is sufficient for a given cyclotron frequency. In other words, what is the smallest betatron tune at which the elastic restoring force is stronger than the imposed shear? As shown in Figure 14, this is a function of the particle number, and for a betatron tune of 2.5 (typical of all the rings under consideration) the system will not survive the shear without slipping. Only for a very large ring, or very strong focusing, such as RHIC with a betatron tune of 30, would larger systems survive without slipping.

PROBLEMS AND POSSIBLE SOLUTIONS

The problems associated with attaining the ordered patterns seen in the MD model calculations are associated with the real features of the storage rings. Three of the major problems are:

a) the shear associated with rotation, that was mentioned above,

b) the fact that the focusing lattice of an accelerator is not constant in time but consists of a series of focusing elements,

c) that the cooling in a storage ring is not constant, but is applied only once per revolution, and that cooling forces act only in the direction of the beam and not three-dimensionally as was done in the MD calculations discussed so far.

Shear

As has already been discussed, the elastic resistance to shear in the storage rings under consideration is not very great, and thus any but the thinnest beams would continuously undergo such shearing motion. Data from Novosibirsk [13] with cooled proton beams seem to indicate a transition: a sudden onset of noise at about the point in beam current where one would expect a cold beam to deviate from a one-dimensional chain -- it remains to be seen whether this threshold is indeed related to such order, since the stated temperatures (actually, limits on temperature) of the beam may not have been sufficiently low for this configuration to have been attained.

A MD calculation with a beam of finite width was allowed to proceed in which shear was imposed with a magnitude corresponding to a betatron tune of 2.5. This was done while cooling the system only along the direction of motion. The system settled only very slowly, and gradually a pattern of longitudinal threads emerged, as shown in Figure 15. The particles are still roughly along the cylindrical layers seen in the static case, but they are segregated into individual strings to minimize their interaction as they slip past each other. It is interesting to note that the arrangement between these strings is again a hexagonal one, presumably because of the repulsive interaction between them. This implies, however, that such a pattern can only be obtained for discrete values of particle currents, and indeed as is also shown in Figure 15, a different number of particles per unit length settles into a pattern that is not so ordered, with threads developed only along a part of the circumference. It thus seems that with a strong (perhaps unrealistically so) cooling force, a form of order may also be obtained in a sheared system.

Two other possibilities remain. If one could introduce a slight gradient in the cooling, to have particles on the outside travelling somewhat faster than those on the inside, then this shear would be absent. Since the magnitude of the shear constant is almost sufficient to withstand the imposed shear, as was seen in Figure 14, the cancellation need not be exact. The electron beams used in cooling do, in fact, have a parabolic velocity profile, and by causing the ion beam to traverse the larger electron beam off center, one may perhaps introduce a gradient in the cooling. Thus it might become possible to find cooling mechanisms that prepares the beam with a velocity gradient to remove, or at least substantially reduce, the effects of shear.

Alternatively, if the beam could be induced to rotate about its own axis, path differences for different particles would disappear for a rotational frequency that is the same as (or an integral multiple of) the cyclotron frequency. It is not clear whether such rotation could be induced; it would imply centrifugal forces on the beam particles that are comparable to the effects of space charge.

Periodic Cooling

The fact that the beam is not cooled as ideally as was assumed in the MD program needs to be considered. First of all the "cooling force" from either laser or electron cooling is applied only along the direction of the beam, second, it is applied generally over only a short stretch along the trajectory. Figure 16 shows the rate of cooling for a system where the particles were cooled only along the beam direction and the "cooling" mechanism applied at only one time step out of 150, which roughly corresponds to the 'once-a-turn' cooling in a ring. It is clear that the system will be cooled somewhat more slowly in this fashion, but once the particles are sufficiently close to interact with each other the transverse and longitudinal degrees of freedom are closely coupled, on a time scale that is comparable to the macroscopic natural frequencies (e.g. the betatron frequency or the plasma frequency of the system) and cooling along one direction causes no problems by itself.

What has not been considered, is the detailed nature of the cooling force, although some estimates by I. Hoffman imply that the approximation used here may not be too bad for a fully stripped uranium beam that has reached the temperature regime where it is space-charge limited: $\Gamma > \sim 0.1$. The MD method is not well suited for considering particles hotter than that, since velocities become large and the size of time steps would have to be reduced requiring prohibitive amounts of CPU time.

Alternating Focusing

Another serious limitation in real storage rings is the fact that particles are contained by the fluctuating focusing fields of an accelerator lattice rather than then constant focusing assumed so far. Simulating a detailed accelerator lattice would require MD calculation with much smaller time steps; the time steps used so far correspond to about 150 per accelerator period and an order of magnitude finer steps would be required. Instead, what has been done is to introduce a time dependence such that the focusing field was turned on and off for alternate equal intervals, out of phase in the horizontal and vertical directions at a rate corresponding to ~15 times per cyclotron orbit. One may perhaps argue that the sharper time variations in a real lattice may not cause additional qualitative problems since the natural radial modes of the system have periods that are of the same order of magnitude as the cyclotron period.

When such a periodic focusing field is introduced for a previously well-ordered beam, it starts to oscillate quite violently. If cooling is allowed to act on the beam in the direction of the beam axi . then these oscillations gradually die out as shown in Figure 17, with orresponding beam profiles in Figure 18. The layers first disappear but then the system gradually becomes ordered again. Apparently the system settles into a mode in which the radial layers oscillate coherently and smoothly and the ordering is almost as good as for static focusing. The dashed line in Figure 17 indicates a similar calculation but with cooling applied only once every 150 time steps to simulate the real periodicity of electron cooling, and although the system settles more slowly, it does seem to follow the same pattern. Similar results were obtained with beams that were initially unordered (Γ = 2). One unit of energy in these figures corresponds to the kinetic energy of the system at the nominal condensation point corresponding to Γ = 200.

Some curves are also shown in the figure where the 'once-a-turn cooling' was applied earlier -- to indicate that this would not cause any problems.

STATUS

There are several questions and issues that I would like to review here briefly -- and I fully expect that by the end of this Workshop these questions will either have answers, or we will be able to regard them in new perspectives.

1) How reliable are the Molecular Dynamic calculations in reproducing the properties of confined cold ionic systems?

It is difficult to answer such a question except by specific example. The experimental observations of the beautiful stratified ion clouds reported by the Boulder group [11] last spring seem to confirm the layered structures predicted by MD calculations. The number of shells that are to be expected for a given number of total ions is also confirmed. When the Boulder results first appeared, it seemed a puzzle that they observed roughly cylindrical shells, while the MD calculations kept showing layers over closed equipotential surfaces; for anisotropic confinement spheroidal ones of the type seen in Figure 8. After much trial and error, I decided to follow up on one aspect of the experiment that Drs. Bollinger and Wineland told me about: the presence of heavy impurity ions that would be carried along with the rotating Be^+ cloud, but that would not be visible to the lasers. Indeed, as is shown in Figure 19, the heavier impurity ions seem to form an equatorial belt around the cloud because of the centrifugal force, and the tightening effect of this belt produces cylindrical shells over a substantial length of the cloud. It is possible that the cloud does not rotate at a uniform angular velocity and shear effects, related to the ones shown in Figure 15 for beams, may cause particles to segregate into bands in the curved end caps of the cloud.

Since the MD calculations, both with a harmonic force, and the 'guiding center approximation' used by Dubin and O'Neil [14], have been successful in predicting the observations in ion traps, it seems reasonable to assume that this model will also be useful in predicting properties of particle beams.

2) How much further can such calculations be pursued in order to understand the behavior of particles in a storage ring and to help optimize conditions in existing rings or to design a ring better suited to the observation of such systems?

The brute-force technique of putting in the realistic details of an accelerator lattice and of electron cooling, and computing the properties of a beam is not likely to be sensible with the present generation of supercomputers, since the number of time steps is likely to have to increase by several orders of magnitude. However, many features of the process could be modelled better than has been done so far, and I suspect that considerable quantitative information remains to be extracted from modelling with the MD techniques for these very cold beams. Examples are the spacing of focusing elements to minimize the excitation of radial modes, the question of the placement of cooling sections with respect to the dipole and focusing elements, better understanding of the quantitative aspects of electron or laser cooling, etc.

3) What are the most promising diagnostic techniques for determining how close a particle beam is to being space-charge limited, and then to observe shell structure and the structure within the shells.

If it were possible to detect the radial modes of a beam discussed above, this could be a rather useful technique for determining the temperature regime of the beam. Beyond that, the shell structure may be observable directly, as it was in the Boulder experiments, with fluorescent light. The finer details of structure would have to be observed with diffraction measurements with visible light, which does not seem to be unreasonable considering the size of spacings one has to deal with. But diagnostic techniques that involve the scattering of light would require that the particles not be fully ionized, and this may present some problems at particular facilities and energy regimes.

One can speculate of more farfetched techniques; of extracting the beam and detecting its structure directly, even of superchannelling between two colliding condensed beams.

4) What is the relationship of studies of this state with ion traps and storage rings?

Condensed layered structures have now been observed in ion traps, and many of the features that one is anticipating for storage rings should have their counterpart in these systems. The competition and interplay between the two rather different techniques should have a beneficial effect on the pursuit of our understanding of this new form of condensed matter. There are broader implications of the phenomena associated with this form of matter in other fields, in condensed matter physics, astrophysics, etc.

REFERENCES

[1] E. Madelung, Phys. Zeitschr. 19, 524 (1918); P. Ewald, Ann. der Phys. 64, 253 (1921); P. Debye and ? Hueckel, Phys. Zeitschr. 24, 185 (1923).

[2] W. P. Wigner, Phys. Rev. 46, 1002 (1934).

[3] S. G. Brush, H. L. Sahlin, and E. Teller, Journ. of Chem. Phys. 45, 2102 (1966).

[4] E. L. Pollock and J. P. Hansen, Phys. Rev. A8, 3110 (1973); W. L. Slattery et al., Phys. Rev. A21, 2087 (1980); S. Ichimaru, H. Iyetomi and S. Tanaka, Physics Reports 149 (2 & 3), 91 (1987).

[5] J. P. Schiffer and P. Kienle, Zeitschr. f. Phys. A 321, 181 (1985).

[6] A. Rahman and J. P. Schiffer, Phys. Rev. Letts. 57, 1133 (1986).

[7] D. Habs, MPI-H-1987-V10; R. Hasse, private communication and this conference.

[8] J. D. Lawson, The Physics of Charged Particle Beams, Clarendon Press, Oxford (1977).

[9] J. P. Schiffer, Phys. Rev. Letts. 61, 1843 (1988).

[10] S. L. Gilbert, J. J. Bollinger, and D. J. Wineland, Phys. Rev. Letts. 60, 2022 (1988).

[11] J. J. Thompson, Phil. Mag. S. 6. 7, 237 (1904).

[12] A. Rahman and J. P. Schiffer, Physica Scripta T22, 133 (1988); and Zeitschr. f. Phys. A 331, 71 (1988).

[13] E. N. Demnt'ev et al., Sov. Phys. Tech. Phys. 25, 1001 (1981).

[14] D. H. E. Dubin and T. M. O'Neil, Phys. Rev. Letts. 60, 511 (1988).

Table I. ROUGH CHRONOLOGY OF COULOMB CRYSTALS WITH EMPHASIS ON STORAGE RINGS

EARLY FOUNDATIONS		
1900-1930	Madelung; Ewald; Debye and Huckel; Born	Classical Problem of One-Component Plasma (Coulomb lattice, summations, etc)
1934	Wigner	Quantum-Mechanical Treatment of Electrons in Solids: bcc
INFINITE ONE COMPONENT PLASMAS		
1966	Brush, Sahlin, Teller	Monte Carlo of Classical One Component Plasma: BCC, Phase Transition
1970-s	J. P. Hansen, et al. Slattery et al.	Molecular Dynamics of OCP -- Refined Results
CONDENSATION IN TRAPS		
1977	Malmberg and O'Neil	Discussion of Cold Electrons in a Trap
1981	Bollinger and Wineland	Discussion of Cold Ions in Penning Traps
ORDERED BEAMS IN STORAGE RINGS		
1980	Dementiev, et al	Anomaly Seen in Cooled Proton Beams at Novosibirsk
1984	GSI	Plans for SIS and ESR
1985	Kienle and JS	Suggestion of Crystalline Beams in HI Storage Rings
1985	Aarhus, MPI	Plans for HI Storage Rings
LAYERED STRUCTURES		
1986	Rahman and JS	Confined Cold Ionic Systems Found to Have Layered Structures in MD Studies, Harmonic Confinement (Cylindrical or Isotropic): Shells, Correlation Functions BCC and Hexagonal, Helical Pattern
1987	Habs	Detailed Study of Helical Structure and Analytic Models
1987	JS	Effects of Shear and Periodic Focusing on Beam Crystals
1988	Dubin and O'Neil	Layered Structures Calculated for Penning Trap Confinement
1988	Gilbert, Bollinger, and Wineland	Observe Layers for REAL Ions in Penning Trap

TABLE II. SPACINGS FOR ORDERED COULOMB SOLIDS WITH EXTERNAL CONFINING FORCES.

D_{sh} is the distance between shells, S_p the nearest-ring L bar spacing within a shell, and W_{sh} the width of shells, all in units of "a".

	D_{sh}	S_p	S_p/D_{sh}	W_{sh}(outer)	W_{sh}(2)
one-dim.	1.38	1.74	1.26	0.040	0.094
two-dim.	1.48	1.80	1.22	0.038	0.10
three-dim.	1.49	1.80	1.21	0.046	0.15
bcc ⟨110⟩	1.44	1.85	1.29		
fcc ⟨111⟩	1.48	1.81	1.22		

FIGURE CAPTIONS

Figure 1. Forces on charged particles at equilibrium with a uniform, cylindrically symmetric, F=-kr focusing force. The dashed line represents the force from space charge, the dot-dashed one the focusing force, and the solid line is their sum. The forces also represent those in an ideal spherical confinement geometry.

Figure 2. Results of a MD calculation for a cold, (Γ = 20000) beam with λ=26 in a constant focusing field. The positions of particles are projected onto a plane perpendicular to the axis.

Figure 3. Particles from the outer shell of the system shown in figure 1, plotted as if the plane of the drawing were the mantle of a cylinder.

Figure 4. Positions of particles from a series of single-shell MD calculations, with different particle densities per unit length.

Figure 5. Density profiles of particles at different temperatures for systems with λ = 26, in a uniform focusing field. The upper left profile corresponds to the system shown in Figures 2 and 3. This figure may be compared to Fig. 4.11 of Reference 8.

Figure 6. Two projections of MD calculations for a system with 5000 particles with a three-dimensionally isotropic restoring force. The lower plot is the arrangement of particles in the outermost shell.

Figure 7. Examples of the minimum energy arrangement of systems with few particles in a three-dimensionally isotropic F=-kr potential. Note the appearance of a particle at the origin for the system with 13 ions.

Figure 8. Examples of particle arrangements with anisotropic confining forces. On the left is the arrangement corresponding to a beam held by a vertical force half as strong as the horizontal one. On the right is a system of 2000 particles confined in three dimensions, with the confining force in the vertical direction, half the strength of that in the other two.

Figure 9. Components of kinetic energy for various cold systems plotted as a function of time in units of the $1/\omega_{plasma}$. At a particular time, the particles in one layer are given a linear or rotational velocity in a direction perpendicular to the confining force. For the upper two figures the solid line represents translational kinetic energy along the beam axis (in units of the dimensionless temperature for Γ = 200) and the dashed line is the kinetic energy associated with rotation about that axis. On the lower left the solid line is for translational kinetic energy along the imposed motion and the dashed one is for motion perpendicular to the first, both along the planes; for the lower right the dashed line is for rotational and the solid for radial kinetic energy.

Figure 10. The value of the average radius of a $\lambda=26$ beam, initially confined by a constant force, with the force turned off for .08 units at time=20. The plot shows the average radius of the system in a MD calculation as a function of time. The subsequent oscillation in average radius was used to determine the period of the radial oscillations.

Figure 11. The dependence of the radial oscillation period as a function of particle density λ is shown by x-s, that for a shape oscillation between a vertically and horizontally deformed beam is shown by ±s.

Figure 12. The dependence of the period of the two modes shown in figure 11 as a function of beam temperature for $\lambda=26$. The initial systems are the ones whose beam profiles were shown in Figure 5.

Figure 13. A system of particles with $\lambda=3$ where a shear has been applied. The shear motion of the system extracted from the MD simulation is plotted as a function of time.

Figure 14. The frequency of shear oscillation as a function of particle density λ in beams confined in a static focusing field. The upper hatched strip represents the approximate ring frequency for several storage rings; the lower one that for the proposed RHIC ring. The error bars represent the estimated accuracy with which these frequencies can be extracted from the damped oscillations of the MD system. The value of λ where the hatched region is crossed by the dashed line drawn to connect the points, represents the estimate of the elastic limit against shear in a condensed beam; for larger values of λ the particles would slip with a unidirectional shear velocity with respect to their neighbors under the forces imposed by the bending magnets of the storage ring.

Figure 15. Results of MD calculations for systems subjected to shear along the axis with a gradient along the bend direction, to simulate bending in the dipoles of a storage ring. The segregation of particles into strings seems to be favored by having an appropriate particle density, as may be seen from the comparison of the top two figures. The bottom section is the radius of particles in the outer shell, indicating a fluctuation in that radius that emphasizes the hexagonal arrangement between strings.

Figure 16. Time required to cool a system of particles when cooling is applied periodically only along the the axis. The idealized cooling, when applied, renormalizes the average kinetic energy of particles in this direction to a prescribed average value. The point on the right would correspond to once-a-turn cooling for a betatron tune of 2.5. The time plotted is that required to go from Γ = 4 to Γ = 20.

Figure 17. Data from a MD model calculation that started cold, with static focusing; the top left of Figure 5. The focusing was changed at time=0 to have a simple time dependence: the field was on (at double the static value) and off for alternate .08 time units, out of phase in the horizontal and vertical directions; cooling was applied only along the axis. On the bottom, the shape oscillations of the beam are shown as a function of time. The solid curve on the top shows

the heat removed from the system, the dashed line is the same quantity when the cooling is applied somewhat more realistically at time intervals corresponding to once per orbit. The dotted line shows the corresponding heat content of the system with no cooling.

Figure 18. Beam profiles corresponding to the system whose properties are shown in Figure 17 (steady cooling) at various times.

Figure 19. A system of particles, three-dimensionally confined in the same fashion as the one shown on the right side of Figure 9, but with 500 of the 2000 particles assumed to be heavier in mass. Since confinement in a Penning trap is from a magnetic field, the centrifugal forces keep these particles in a belt around the equator of the cloud, but this belt has the effect of slimming the lighter ion configuration into a near-cylindrical shape that is closer to that observed experimentally [10].

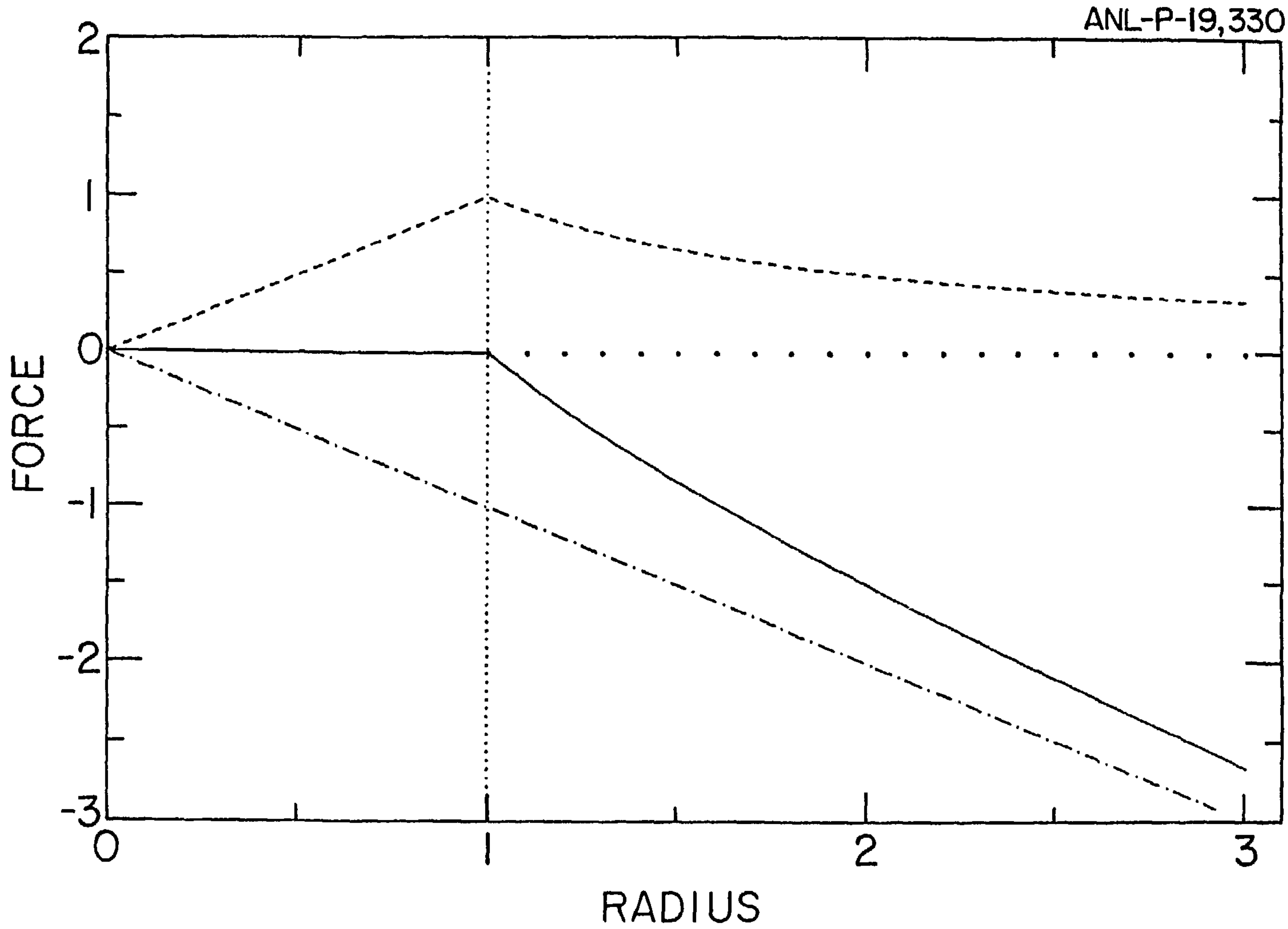

Fig. 1

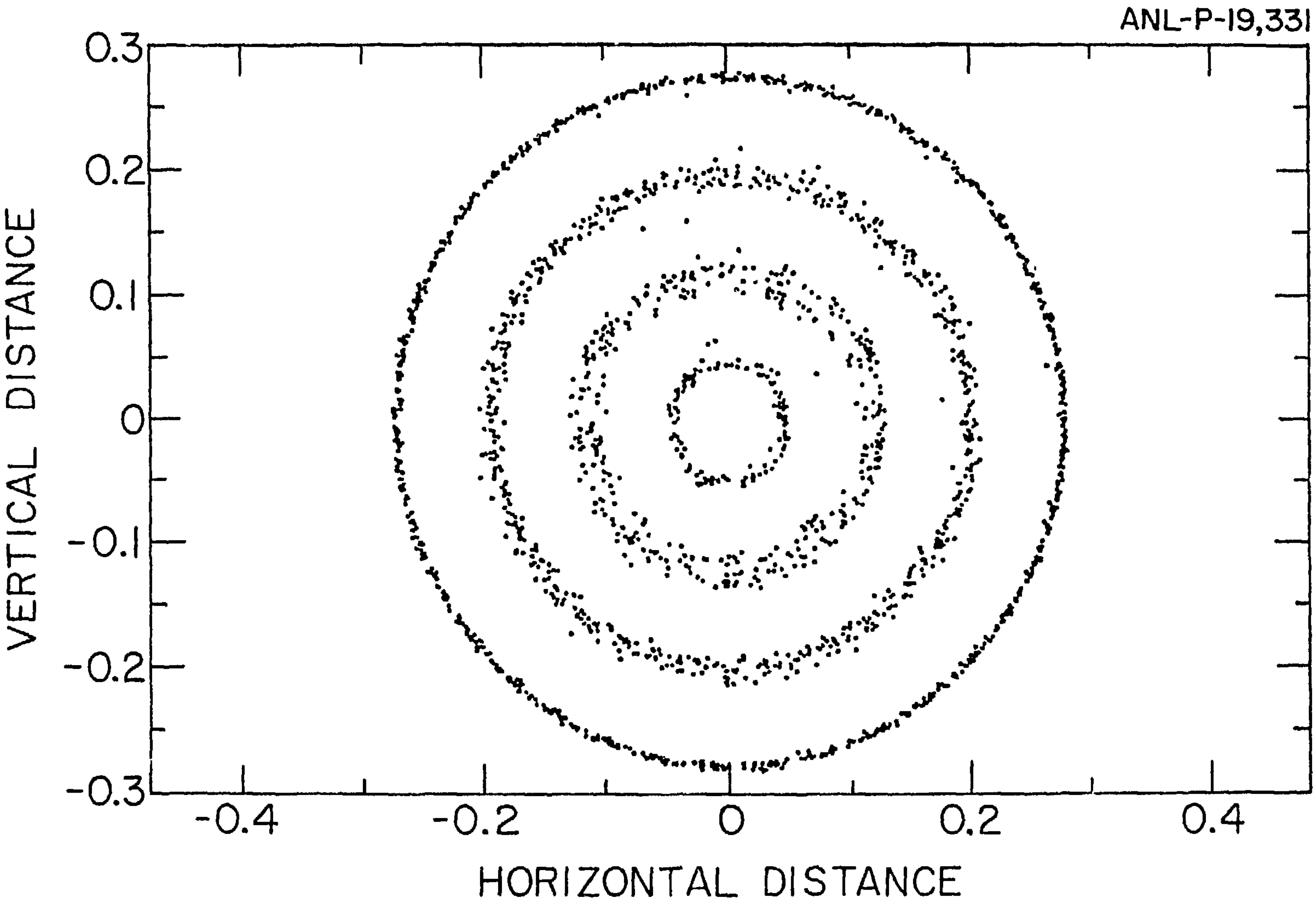

ANL-P-19,331
0.3
0.2
0.1
0
-0.1
-0.2
-0.3
VERTICAL DISTANCE
-0.4
-0.2
0
0.2
0.4
HORIZONTAL DISTANCE

Fig. 2

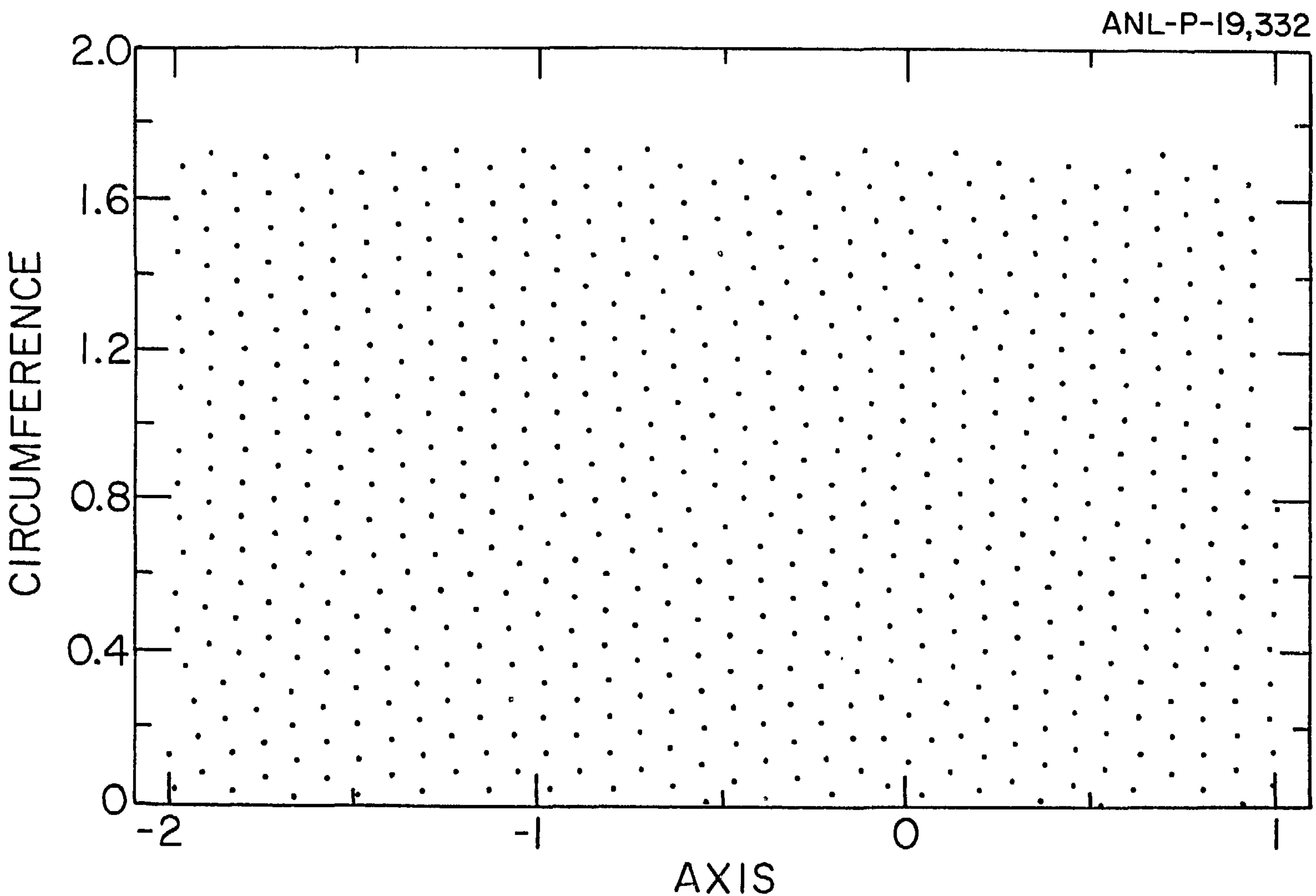

Fig. 3

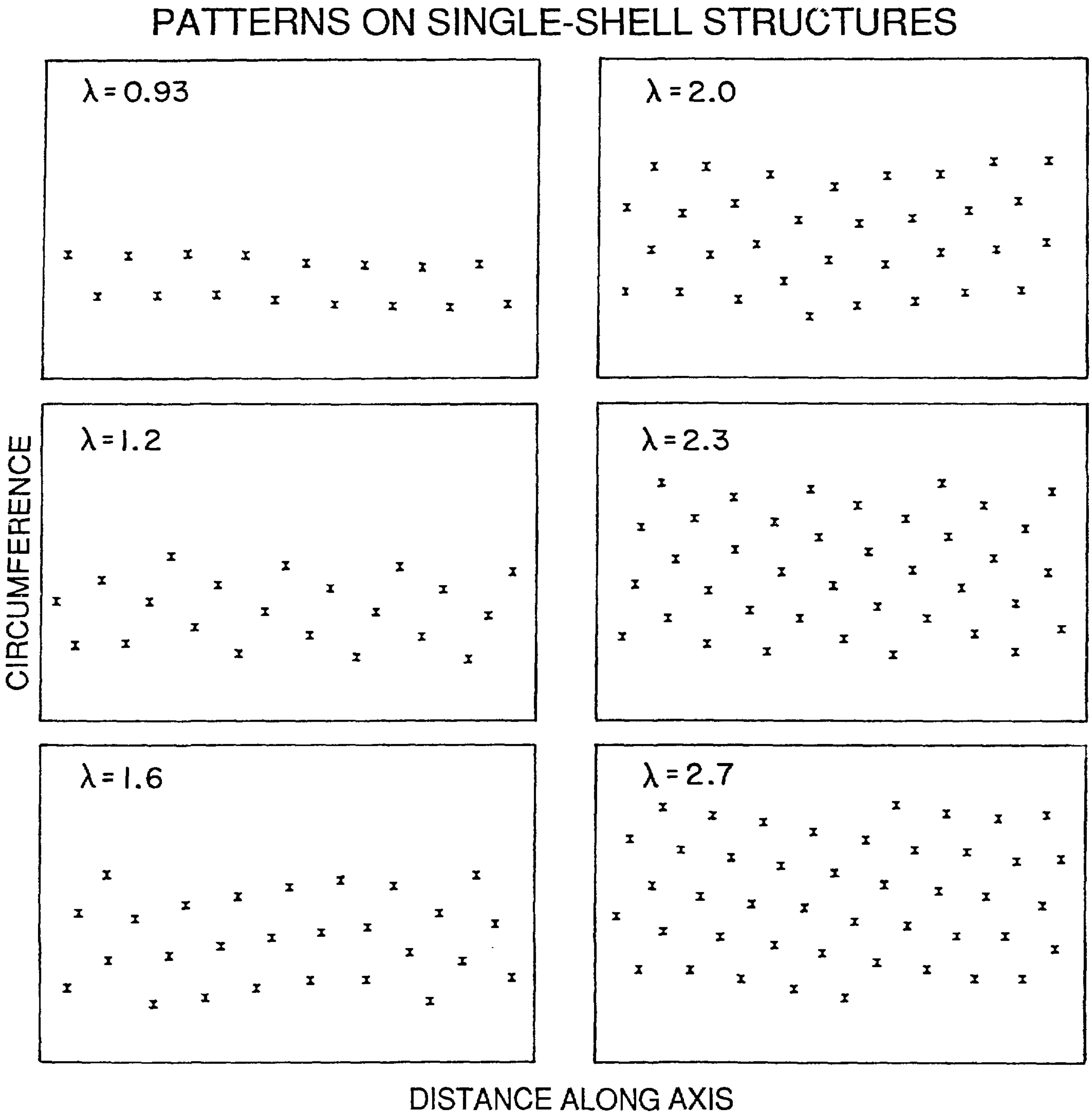
PATTERNS ON SINGLE-SHELL STRUCTURES
λ = 0.93
λ = 2.0
λ = 1.2
λ = 2.3
λ = 1.6
λ = 2.7
CIRCUMFERENCE
DISTANCE ALONG AXIS

Fig. 4

RADIAL DENSITY AT DIFFERENT TEMPERATURES

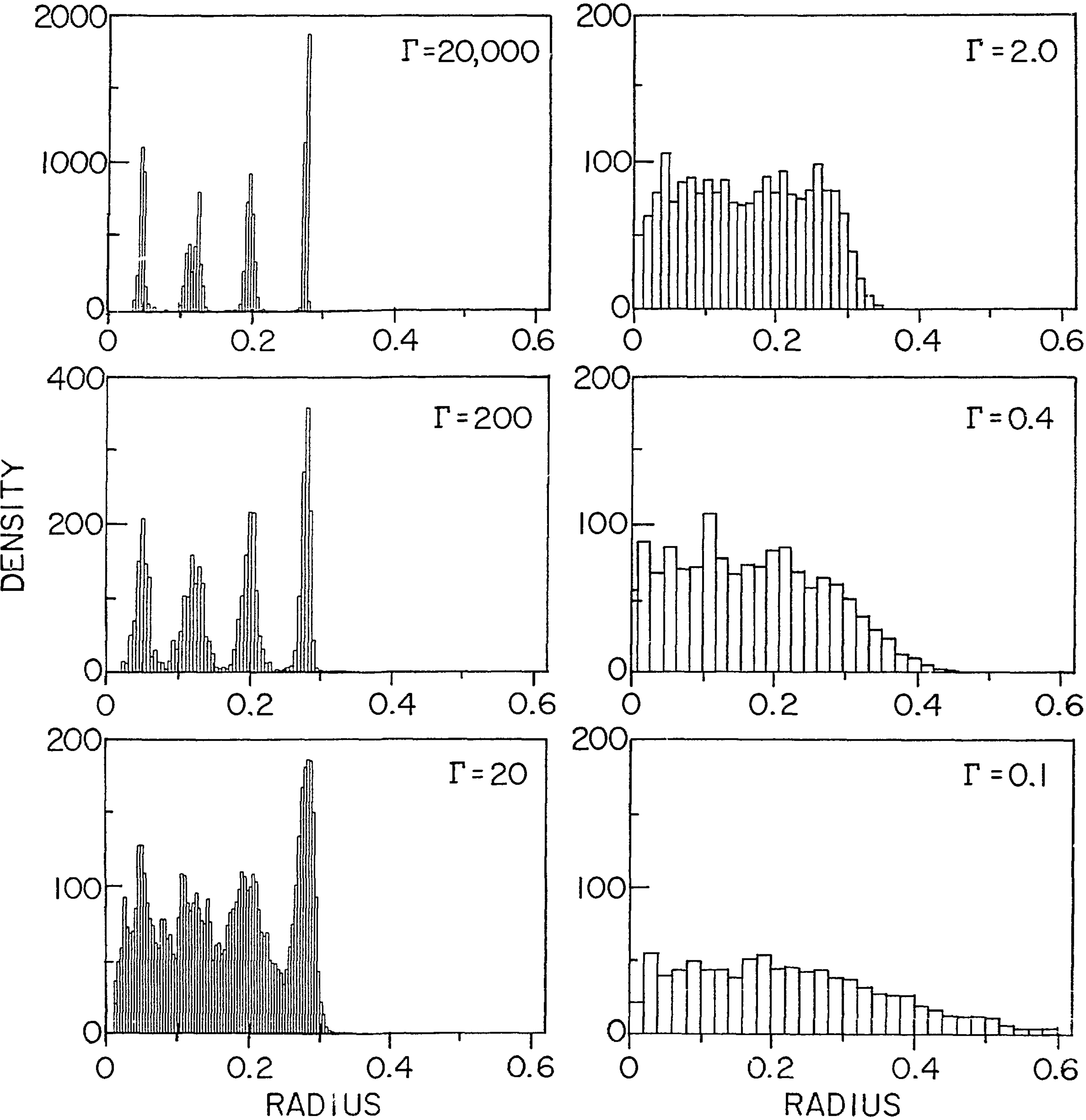

ANL-P-19,333

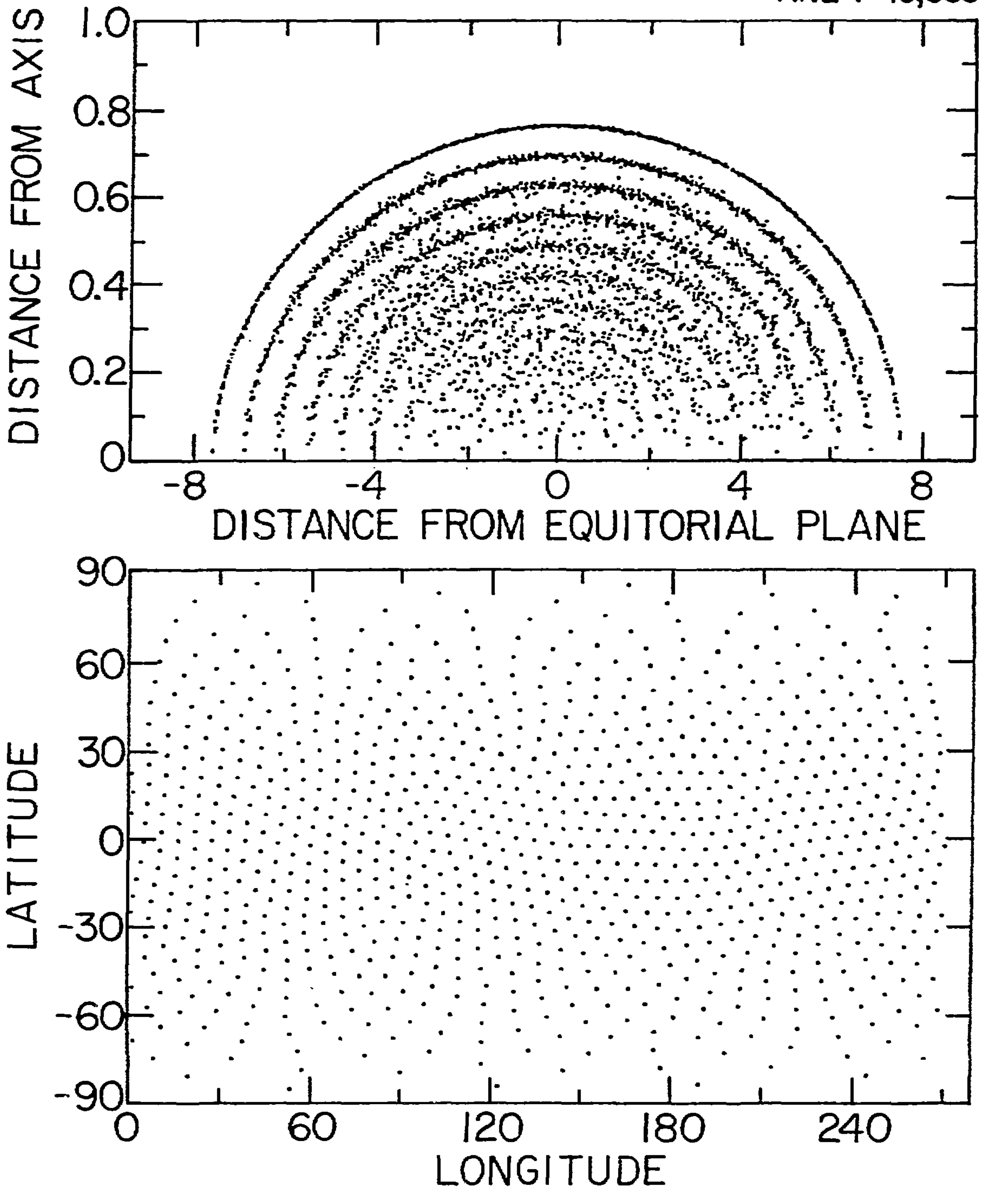
DISTANCE FROM AXIS
1.0
0.8
0.6
0.4
0.2
0
-8
-4
0
4
8
DISTANCE FROM EQUITORIAL PLANE
LATITUDE
90
60
30
0
-30
-60
-90
0
60
120
180
240
LONGITUDE

FEW PARTICLES IN ISOTROPIC CONFINEMENT

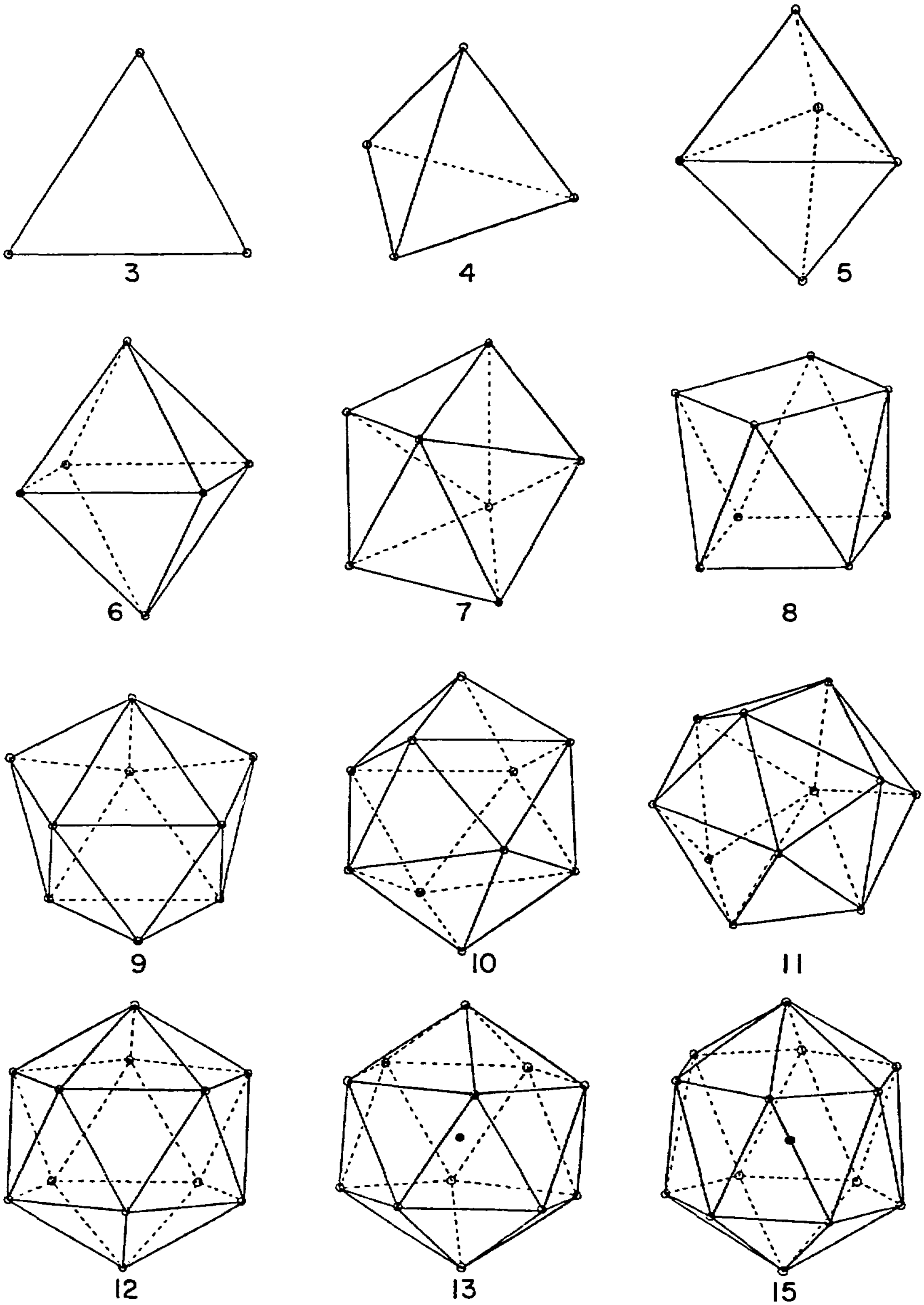

Fig. 7

ANL-P-19,334

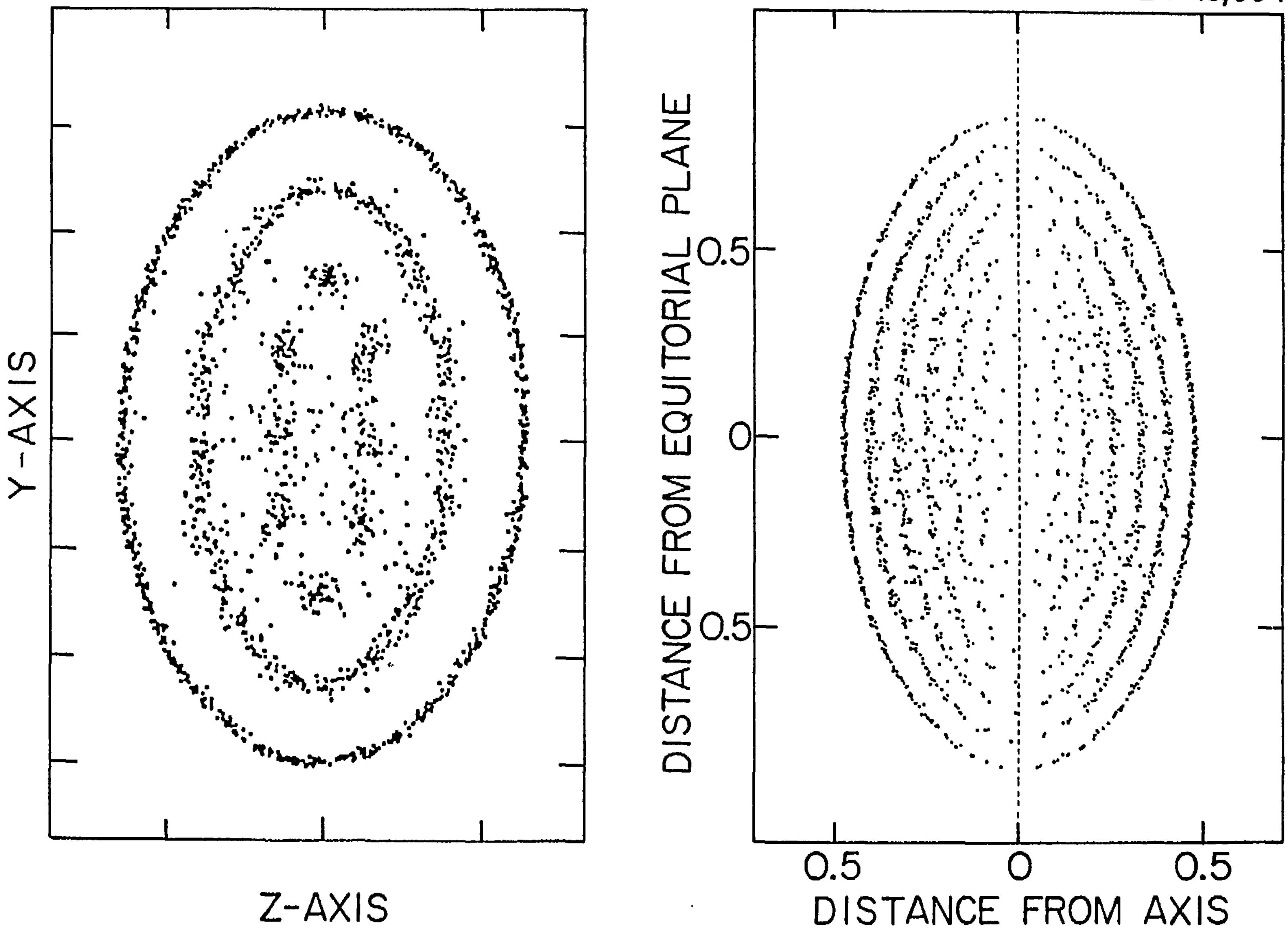

Fig. 8

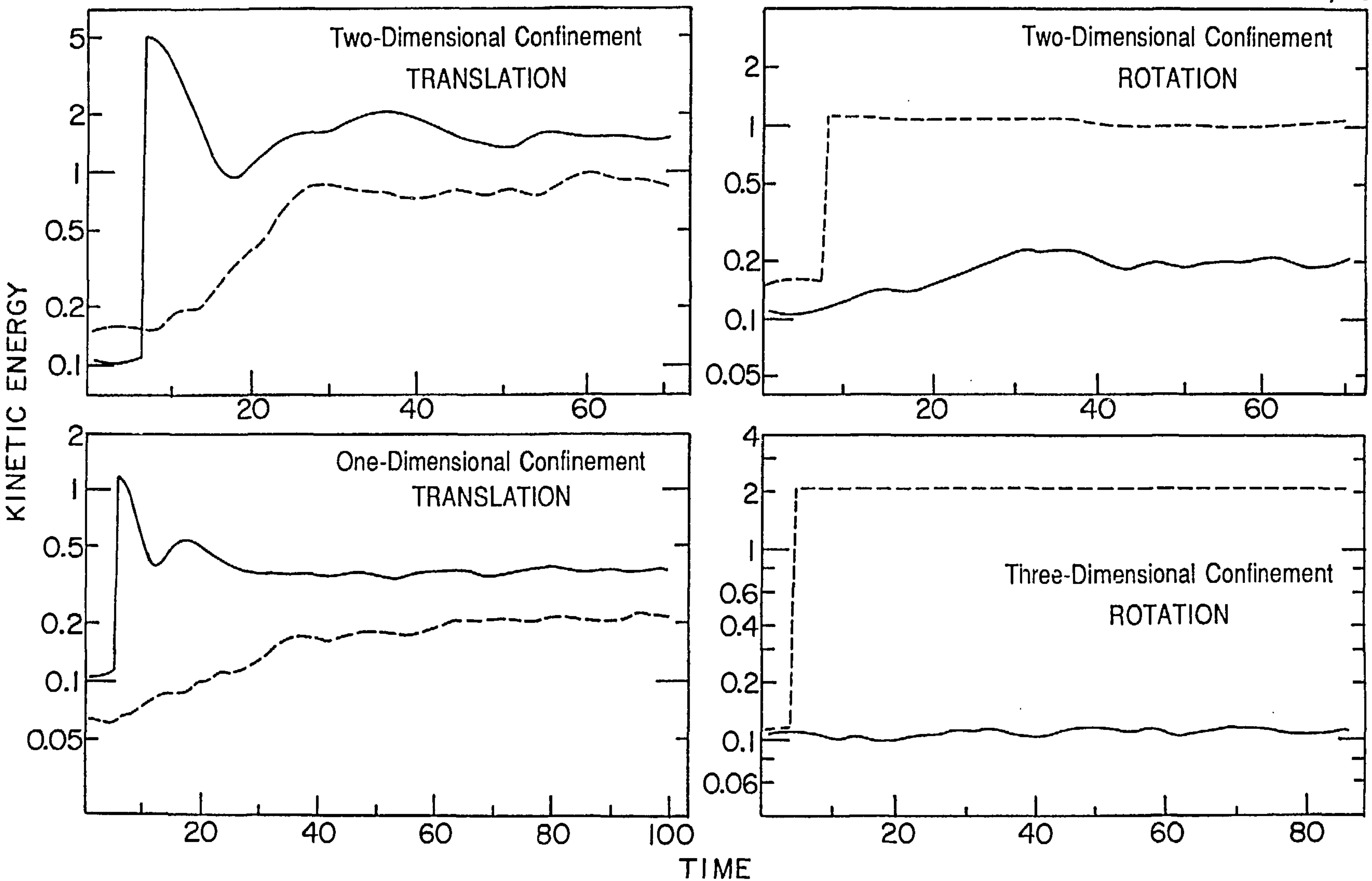
Two-Dimensional Confinement
TRANSLATION
Two-Dimensional Confinement
ROTATION
One-Dimensional Confinement
TRANSLATION
Three-Dimensional Confinement
ROTATION
KINETIC ENERGY
TIME
5
2
1
0.5
0.2
0.1
0.05
0.06
0.4
0.6
4
20
40
60
80
100

Fig. 9

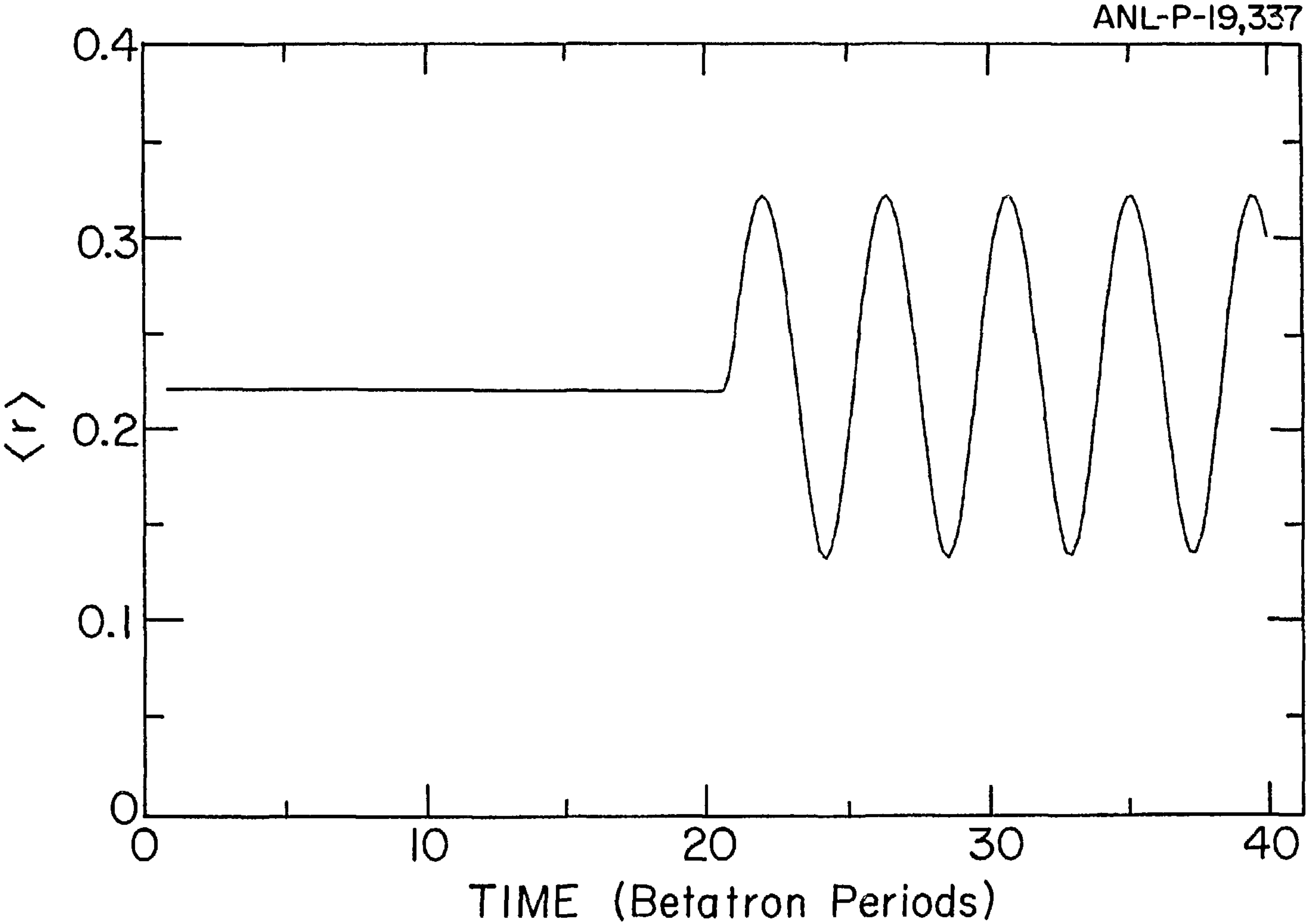

Fig. 10

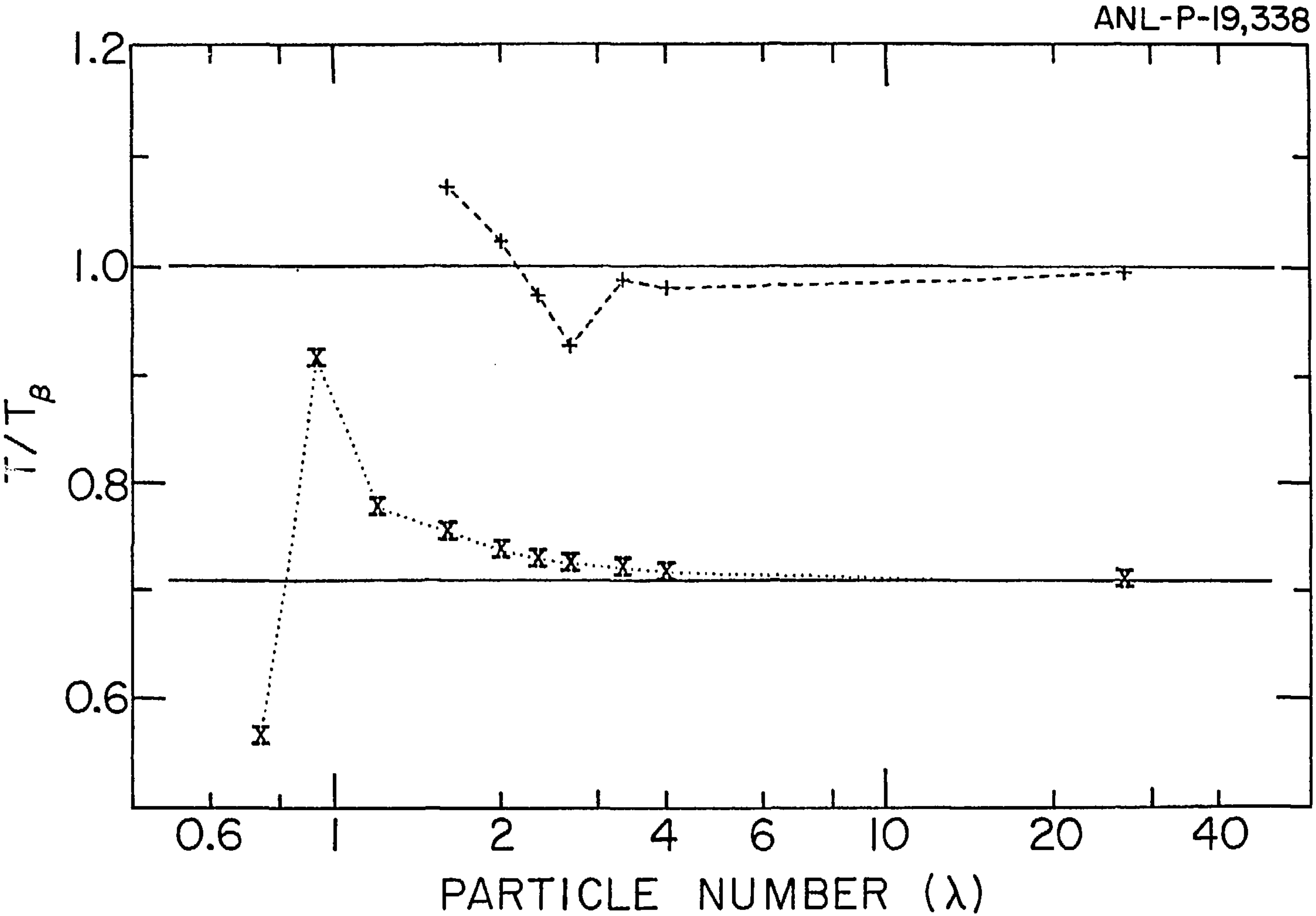

Fig. 11

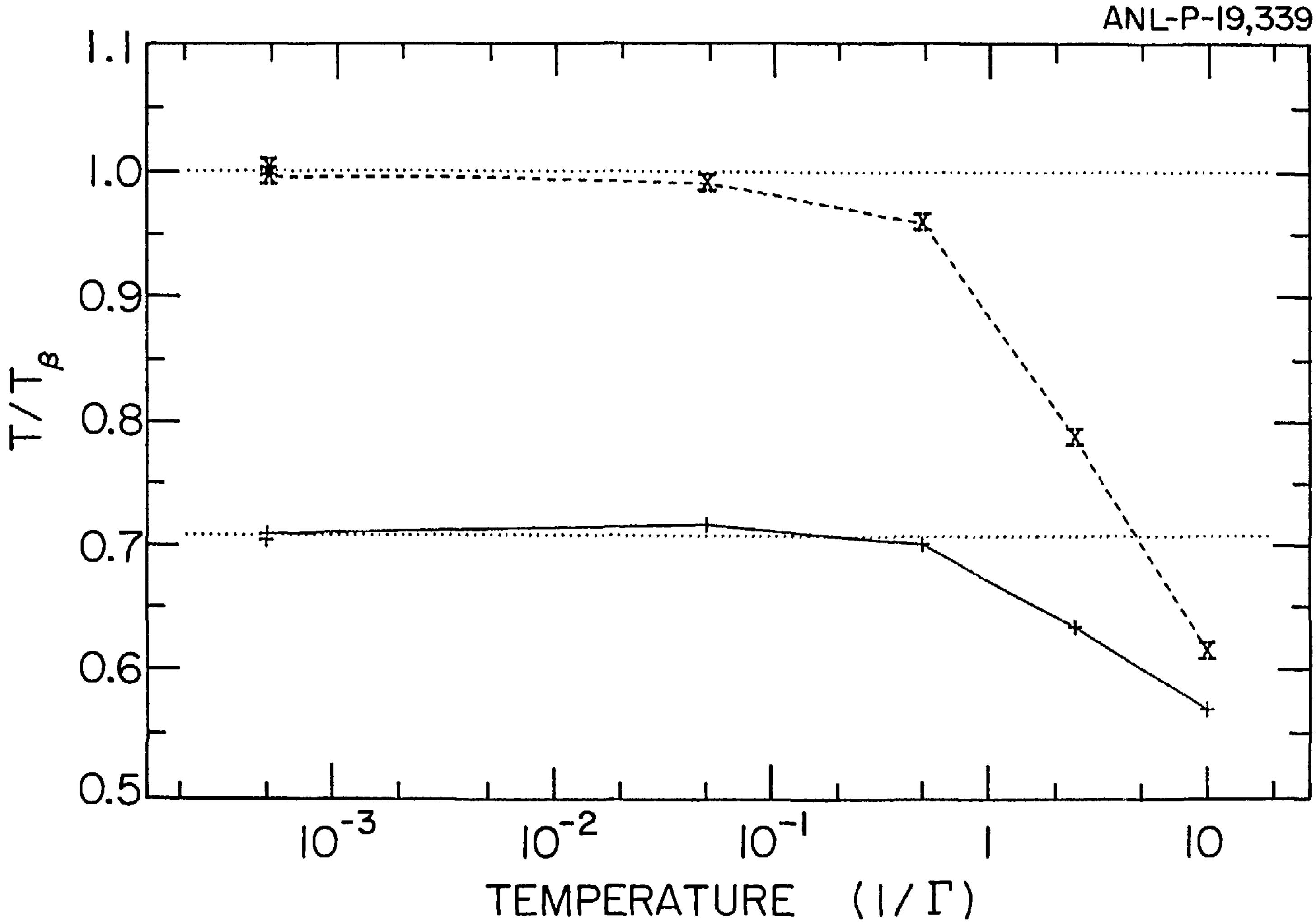
ANL-P-19,339
1.1
1.0
0.9
0.8
0.7
0.6
0.5
T/T_β
10^{-3}
10^{-2}
10^{-1}
1
10
TEMPERATURE (1/Γ)

Fig. 12

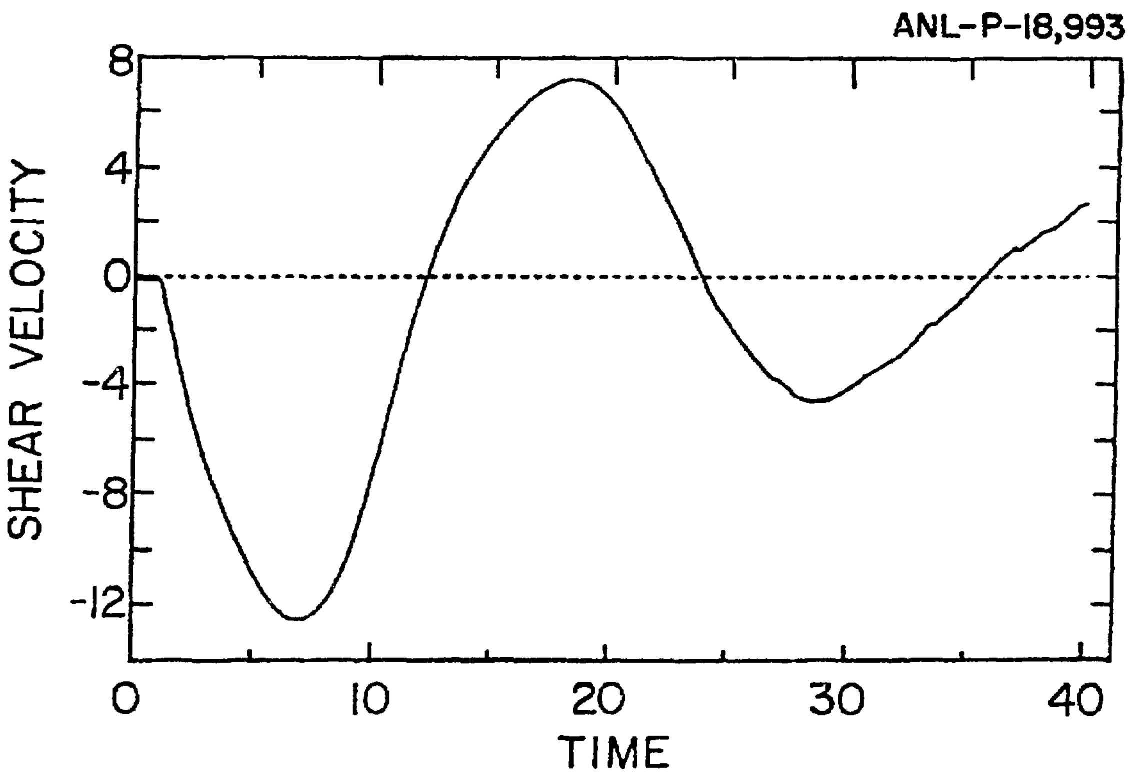

Fig. 13

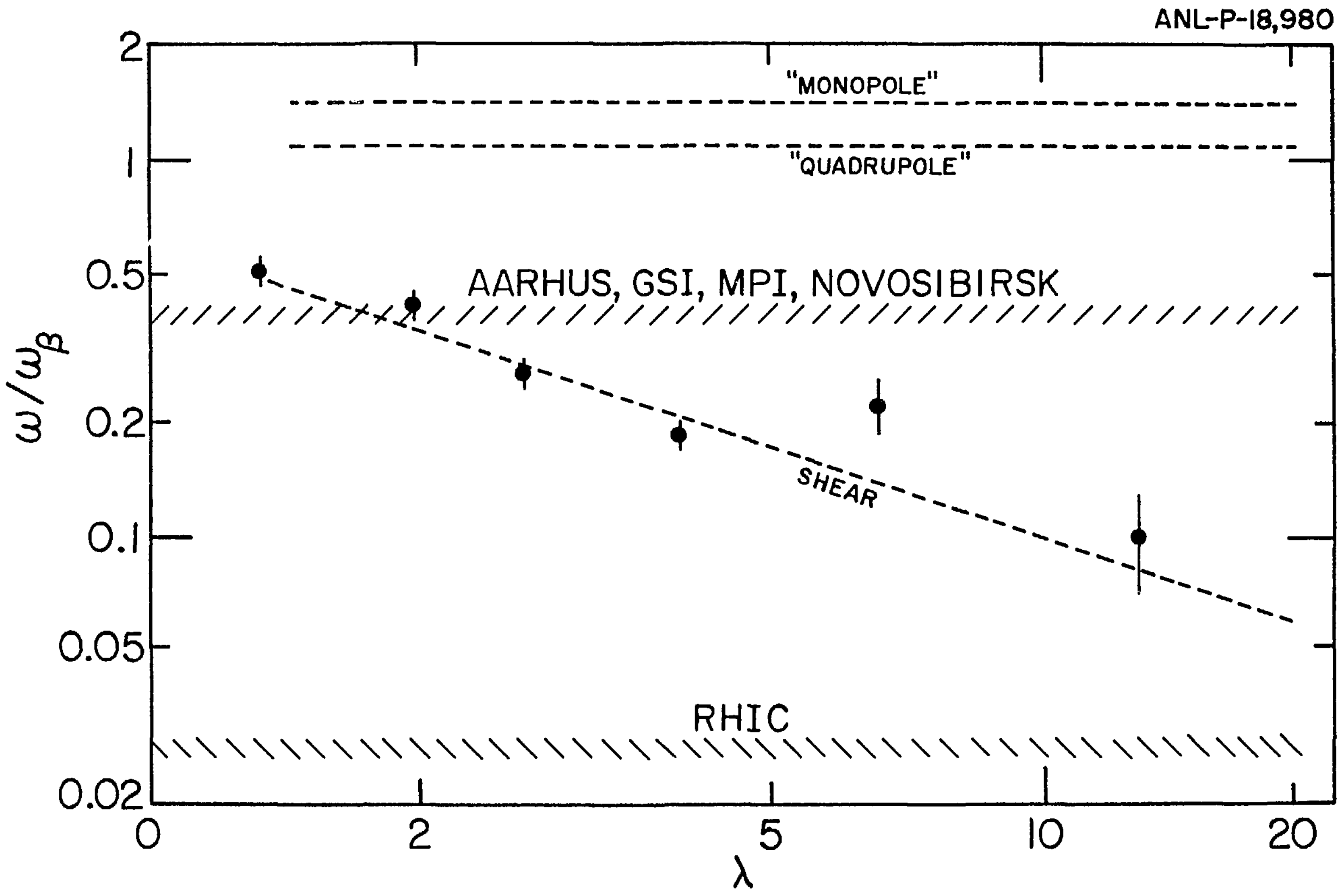

ANL-P-18,980
"MONOPOLE"
"QUADRUPOLE"
AARHUS, GSI, MPI, NOVOSIBIRSK
SHEAR
RHIC
2
1
0.5
0.2
0.1
0.05
0.02
0
2
5
10
20
λ
ω/ω_β

Fig. 14

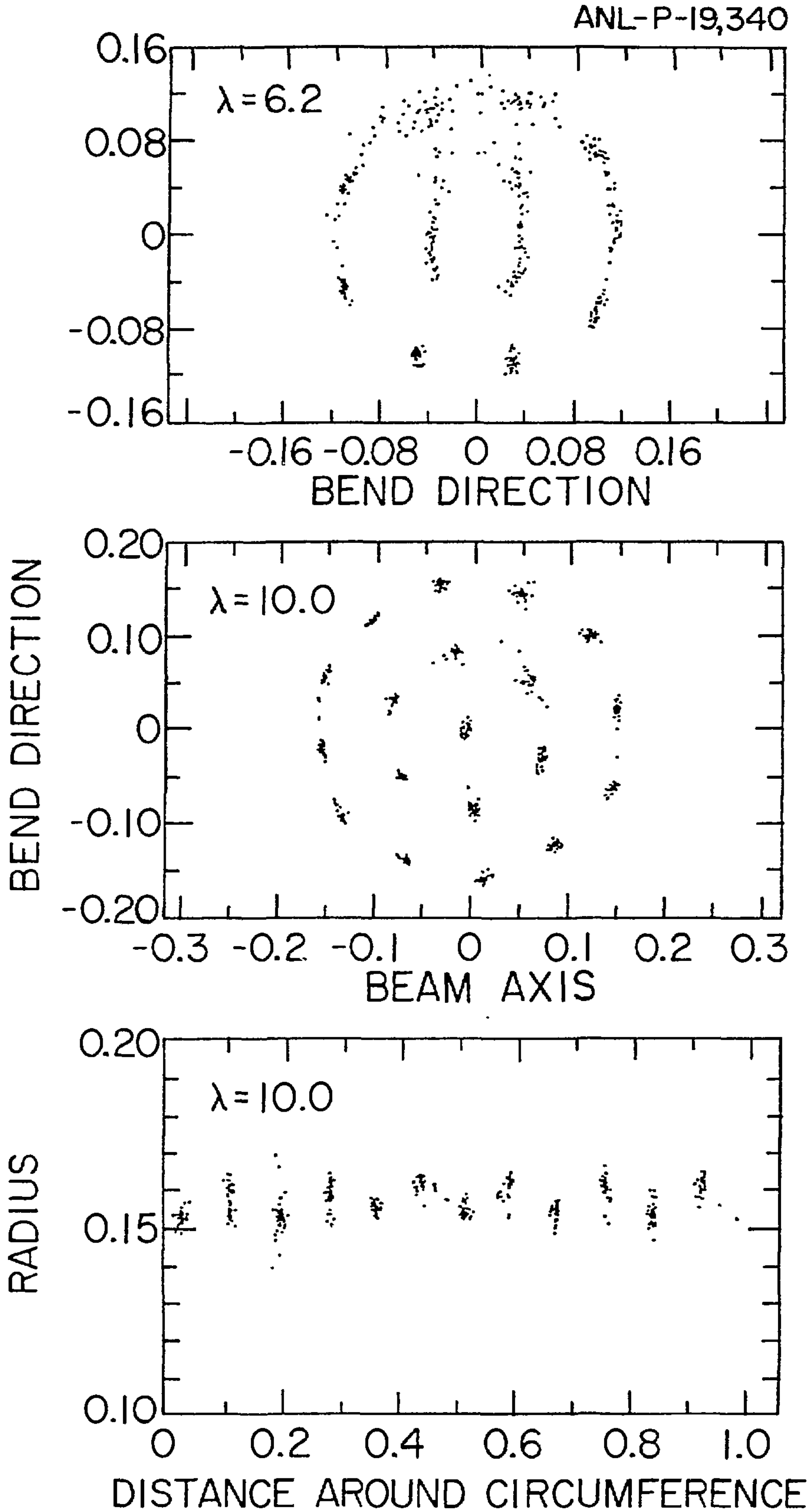

ANL-P-19,340
λ=6.2
0.16
0.08
0
-0.08
-0.16
-0.16 -0.08 0 0.08 0.16
BEND DIRECTION
λ=10.0
0.20
0.10
0
-0.10
-0.20
-0.3 -0.2 -0.1 0 0.1 0.2 0.3
BEAM AXIS
BEND DIRECTION
λ=10.0
0.20
0.15
0.10
0 0.2 0.4 0.6 0.8 1.0
DISTANCE AROUND CIRCUMFERENCE
RADIUS

Fig. 15

ANL-P-19,325

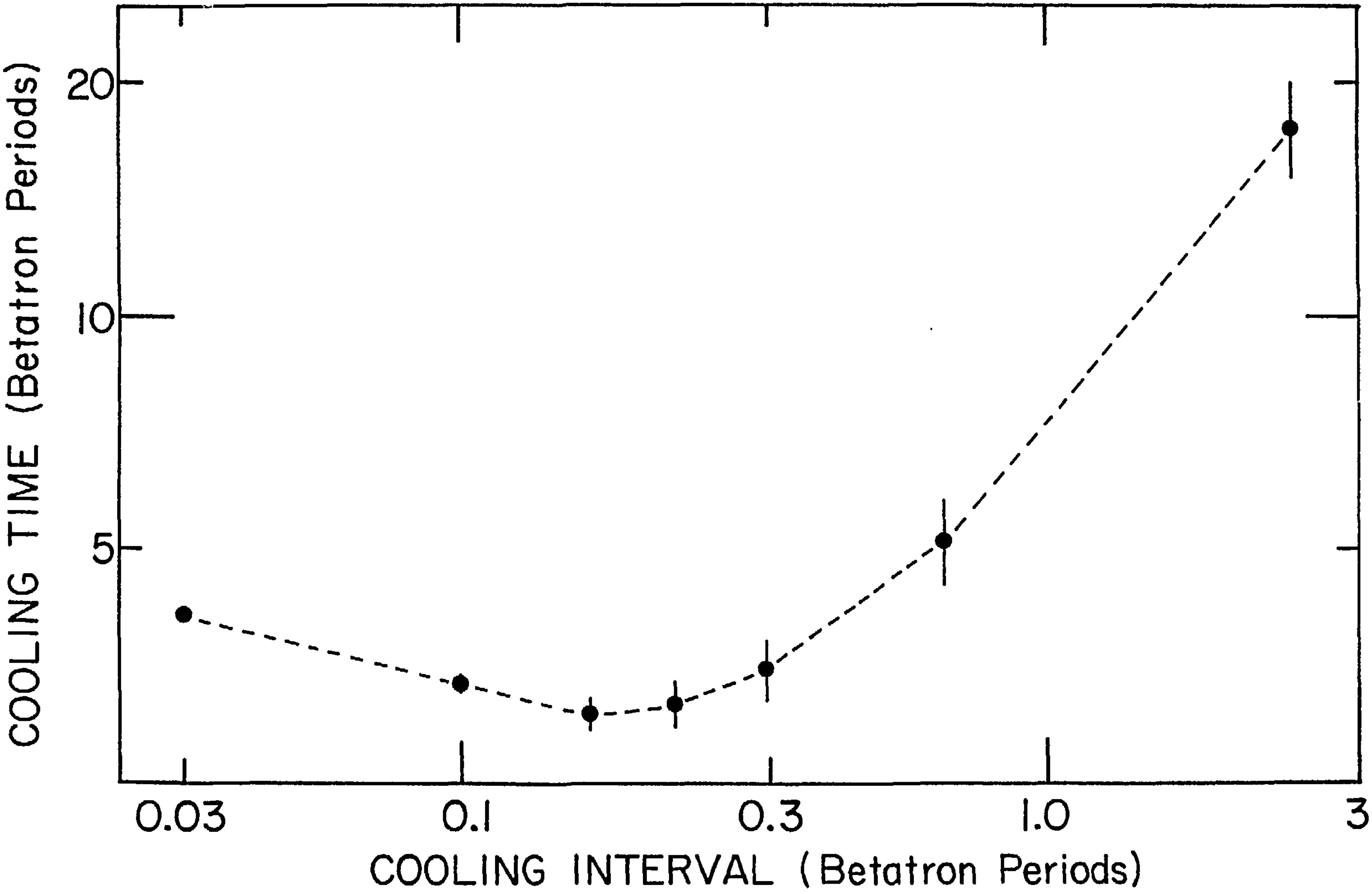

Fig. 16

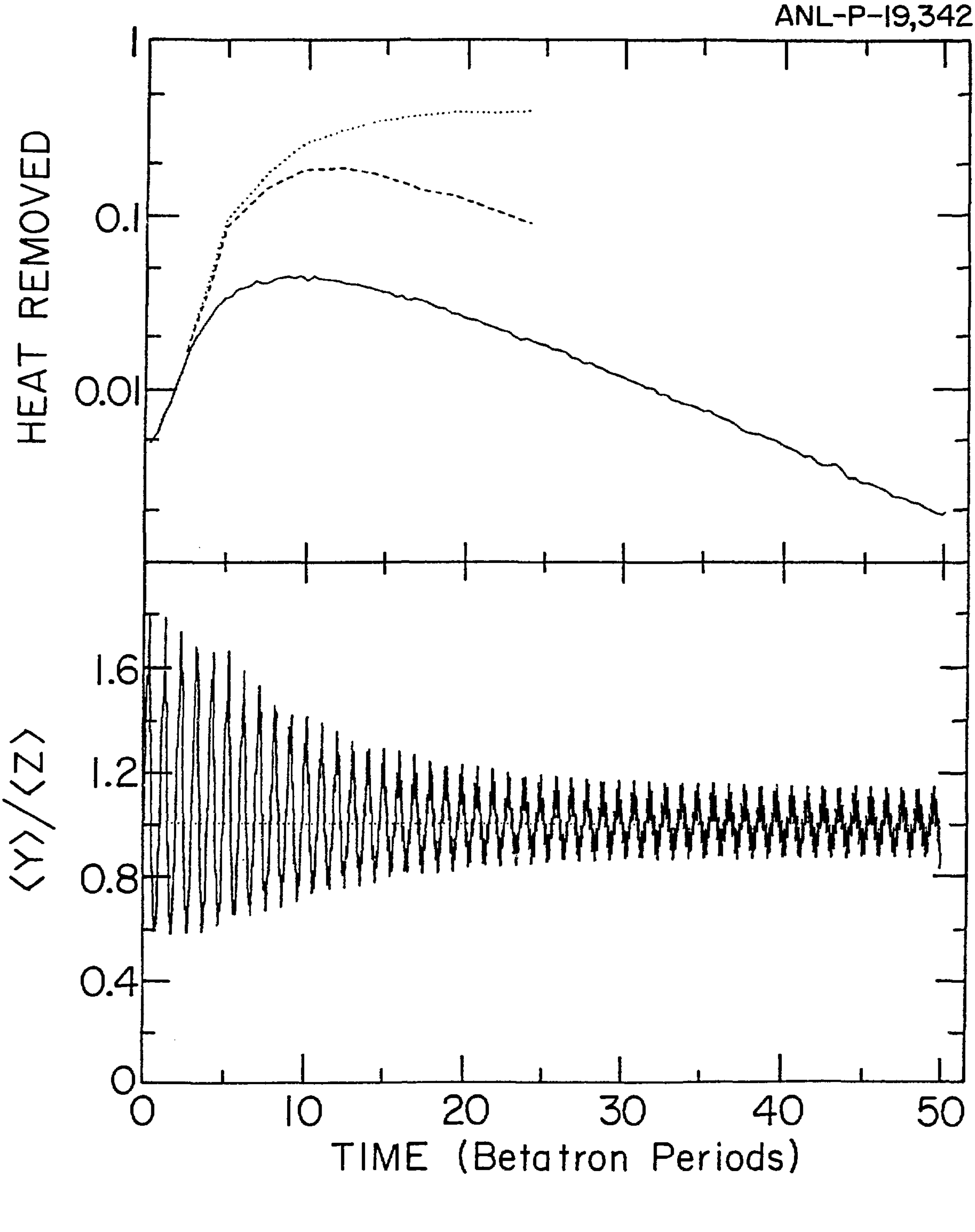
ANL-P-19,342
HEAT REMOVED
1
0.1
0.01
⟨Y⟩/⟨Z⟩
1.6
1.2
0.8
0.4
0
0
10
20
30
40
50
TIME (Betatron Periods)

Fig. 17

TIME DEVELOPMENT OF BEAM PROFILE WITH ALTERNATING FOCUSING AND COOLING ALONG BEAM

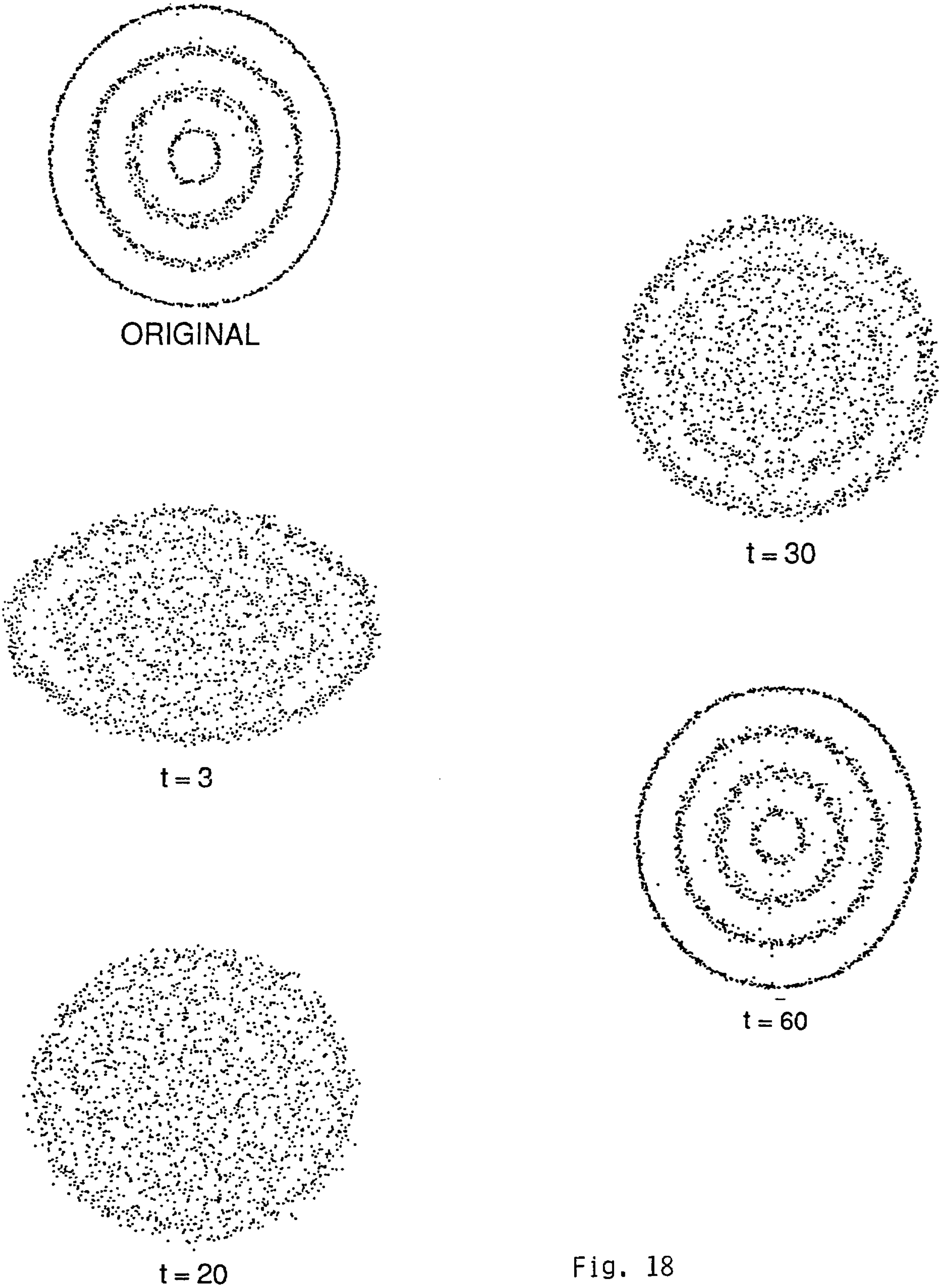

Fig. 18

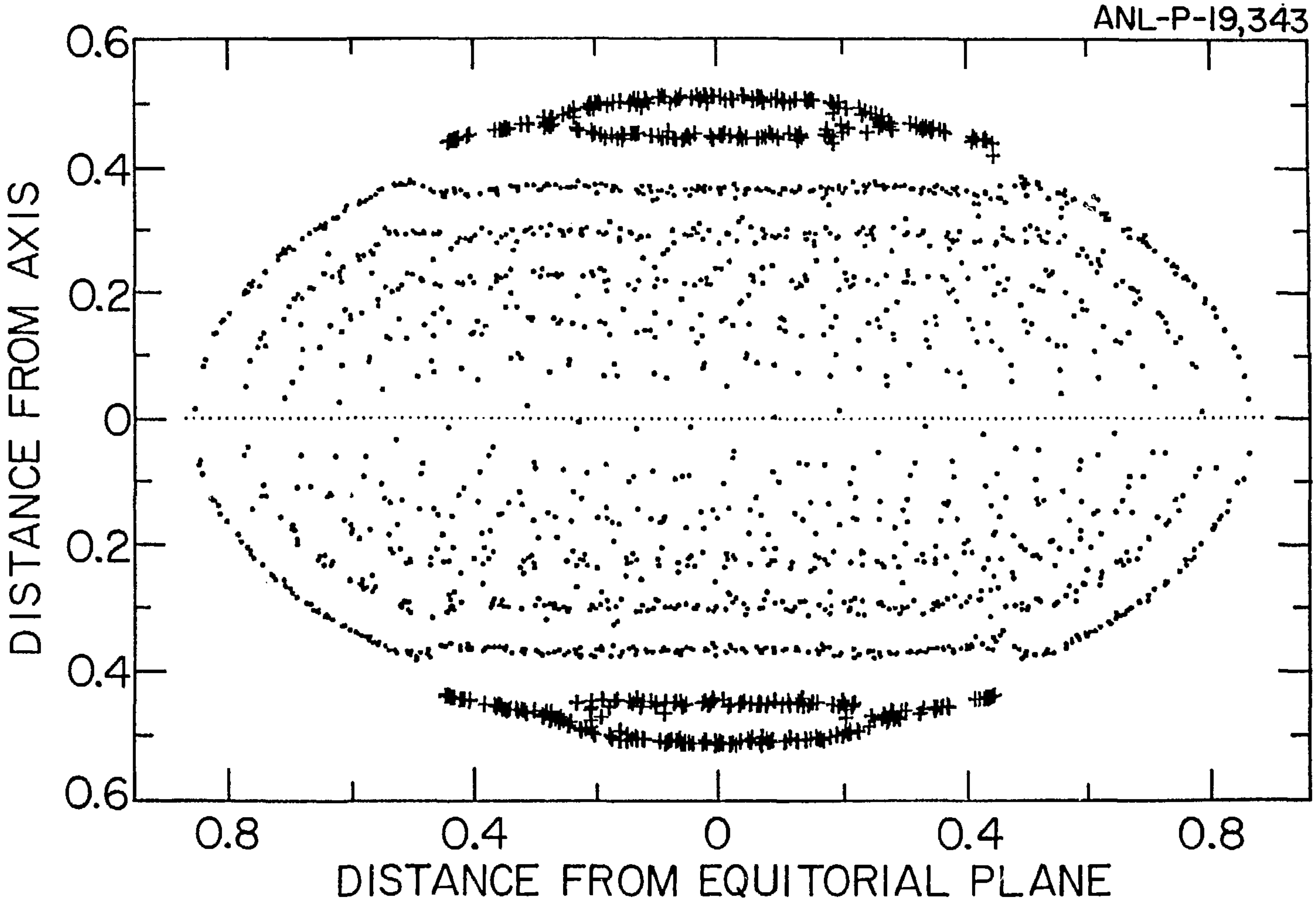

ANL-P-19,343
0.6
0.4
0.2
0
0.2
0.4
0.6
DISTANCE FROM AXIS
0.8
0.4
0
0.4
0.8
DISTANCE FROM EQUITORIAL PLANE

Fig. 19